Hindawi
Journal of Advanced Transportation
Volume 2018, Article ID 2713868, 10 pages
https://doi.org/10.1155/2018/2713868

Research Article

An Earlier Predictive Rollover Index Designed for Bus Rollover Detection and Prevention

Shun Tian,[1] **Lang Wei**,[1] **Chris Schwarz**,[2] **WenCai Zhou**,[1] **Yuan Jiao**,[3] **and YanQin Chen**[4]

[1]*School of Automobile, Chang'an University, Xi'an 710064, China*
[2]*National Advanced Driving Simulator, University of Iowa, Iowa City 52242, USA*
[3]*School of Construction Machinery, Chang'an University, Xi'an 710064, China*
[4]*Department of Mechanical Engineering, Inha University, Incheon 2212, Republic of Korea*

Correspondence should be addressed to Lang Wei; qch_l@chd.edu.cn

Received 29 July 2018; Accepted 11 October 2018; Published 1 November 2018

Guest Editor: Petru Andrei

As vehicle rollovers annually cause a great deal of traffic-related deaths, an increasing number of vehicles are being equipped with rollover prevention systems with the aim of avoiding such accidents. To improve the functionality of active rollover prevention systems, this study provided a potential enhanced method with the intention to predict the tendency of the lateral load transfer ratio (LTR), which is the most common rollover index. This will help provide a certain amount of lead time for the control system to respond more effectively. Before the prediction process, an estimation equation was proposed to better estimate the LTR; the equation was validated using Simulink and TruckSim. Further, to eliminate the influence of drawbacks and make this method practical, a buffer operator was added. Simulation results showed that grey LTR (GLTR) was able to roundly predict the future trend of the LTR based on current and previous data. Under the tests of "Sine with Dwell" (Sindwell) and double lane change (DLC), the GLTR could provide the control system with sufficient time beforehand. Additionally, to further examine the performance of the GLTR, a differential system model was adopted to verify its effectiveness. Through the Sindwell maneuver, it was demonstrated that the GLTR index could improve the performance of the rollover prevention systems by achieving the expected response.

1. Introduction

Among traffic issues, bus rollover is a huge problem for bus manufacturing enterprises and traffic administration. To solve this problem, researchers and engineers have developed many kinds of rollover prevention systems [1]. However, once the phase of the impending rollover begins, there is not enough time left for the actuators to act accurately, especially during extremely dangerous situations [2]. Therefore, being able to predict the rollover tendency beforehand and to produce a suitable compensation time are essential for preventing bus rollover situations.

Currently, the load transfer ratio (LTR) is a widely used reference parameter for rollover detection [3], having been used as the rollover index for antirollover bars [4] and differential braking systems [5]. Commonly, a rollover prevention system initiates the actuators once the LTR exceeds a certain threshold. If an algorithm could predict the LTR, then the lead time could increase the gap between the predicted LTR and the actual LTR. As a result, there would be enough time for the actuator to initiate an effective countermeasure, therefore increasing its effectiveness.

There are many kinds of prediction methods used for different purposes [6, 7]. Deep learning methods are commonly used prediction tools, which have been used among many fields including car risk prediction [8]. However, LTR prediction is a real-time process; only the newly transitory acquired data can be used. Therefore, since LTR prediction is a real-time process, a potential prediction algorithm should have the following characteristics: a small sample size, fast computation, and small internal storage requirements. One suitable method is the grey model, coined by Deng in the 1980s [9]. This model is good at solving uncertainty problems with small samples and poor information. Vehicle motion is

a rapid course; therefore, old data is not useful for the real prediction and has a side effect on the results because the data is not new enough. Hence, we developed a grey-model-based prediction method to conduct LTR prediction to form an early rollover index. The grey model has achieved great success in many fields and has been used in offline prediction. Using fatal crash data from the United Kingdom, Mao et al. [10] applied the grey model to future risk estimation and found that the predicted value approached the actual value. The grey model was applied to predict the vehicle's wheel slip, and then the predicted slip was transferred to a sliding mode controller, which strengthened the controller's robustness [11]. The grey model has also been used to predict the lateral distance between approaching vehicles to provide drivers with extra time to react to an impending collision [12]. In terms of real-time LTR simulation, Chou et al. [13] combined a grey model and a rollover index to detect the rollover of a 14-degree-of-freedom tractor-trailer. The results showed that the grey rollover index achieved an earlier detection of the rollover threat than the rollover index alone; furthermore, the lead time was sufficient for the actuator to be involved. However, the vehicle model they used was an ideal Simulink model, which is largely different from a real bus, and its LTR estimation did not match well with the TruckSim LTR. In this study, a more accurate estimation model was used, and the outputs from TruckSim were directly adopted. In addition, to mitigate the LTR's shock data, a buffer operator was employed to ensure the effectiveness of the grey LTR (GLTR) throughout a wider speed range. Furthermore, a rollover prevention system model was built to examine the function of the GLTR.

The main contributions of this paper are the following:

(1) A predictive LTR, which can be regarded as an earlier rollover detection index, was introduced to achieve rollover prediction.

(2) The GLTR was effective at making predictions during two standard handling tests, "Sine with Dwell" (Sindwell) and double lane change (DLC), proving that GLTR can cope with different kinds of lateral motions.

(3) A considerable lead time was generated to increase the working time available for initiating a rollover prevention action.

(4) GLTR index was brought into rollover prevention. The effectiveness in reducing the rollover risks was further verified via TruckSim–Simulink cosimulation by building a differential braking system.

The rest of the paper is organized as follows: Section 2 presents the bus rollover model, tier model, and its LTR estimation. Section 3 introduces the LTR prediction methodology, including the grey model (first-order one variable) known as GM(1, 1), as well as the buffer operator. Section 4 presents the simulation results of the LTR prediction. Section 5 offers a further simulation study, which fused the GLTR with a differential-based braking system. Finally, Section 6 offers our conclusions.

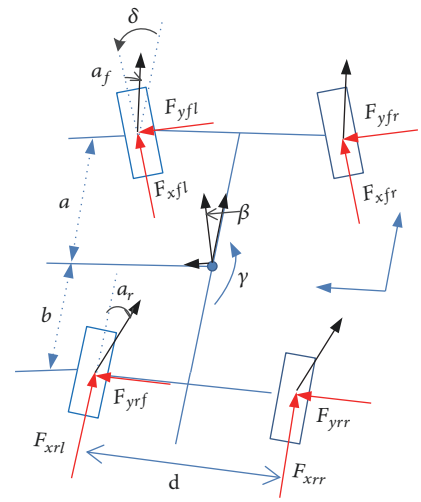

Figure 1: Bus rollover dynamic model.

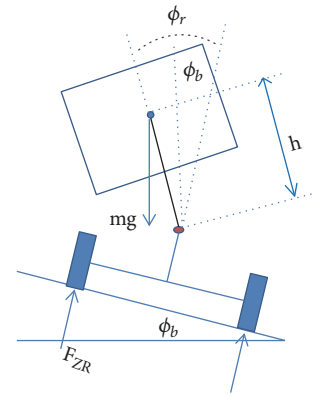

Figure 2: Bus roll dynamics.

2. Bus Dynamic Model

2.1. LTR Estimation. It is not easy to detect the real force acting on tires since the necessary sensors are extremely expensive. Therefore, a bus rollover dynamic model was constructed to establish a suitable LTR estimation equation.

Figure 1 illustrates the lateral dynamics of a bus. The diagram includes the bus yaw angle direction and yaw rate, velocity, and slip angle. Figure 2 shows the roll dynamics of the bus. The effect of the bus's unsprung mass on the roll dynamics was neglected. The road bank angle and the bus roll angle and distance associated with the roll center are also indicated in this diagram.

In Figures 1 and 2, d is the bus width; h is the vertical distance from the sprung mass CG to the assumed roll axis; γ is the yaw rate; ß is the bus's slip angle; δ is the steering wheel angle; $F_{xfl, xfr}$ are the front left and the front right longitudinal forces; $F_{yfl, yfr}$ are the front left and the front right lateral forces; af and ar are the front tire's slip angle and rear tire's angle; and finally, ϕ_b and ϕ_v are the road bank angle and the vehicle roll angle, respectively.

The bus lateral dynamics can be written as

$$\begin{aligned}\sum F_y &= mA_y \\ &= F_{yrl} + F_{yrr} + \left(F_{yfl} + F_{yfr}\right).\cos\delta \\ &\quad + \left(F_{xfl} + F_{xfr}\right).\sin\delta\end{aligned} \tag{1}$$

and

$$\begin{aligned}&\left(I_{xx} + mh^2\right).\left(\ddot{\phi}_r - \ddot{\phi}_b\right) = \left(F_{zL} - F_{zR}\right).\frac{d}{2} \\ &+ \sum F_y.h.\cos\phi_r + mgh.\sin\phi_r.\cos\phi_b \\ &- mgh.\cos\phi_r.\sin\phi_b \\ &+ \left[\left(I_{yy} - I_{zz}\right) - mh^2\right].\gamma^2.\sin\left(\phi_r - \phi_b\right).\cos\left(\phi_r - \phi_b\right)\end{aligned} \tag{2}$$

where $A_y = \dot{v} + ru - g.\sin\phi_b + h\phi_r{}^2.\sin\phi_r + h\gamma^2.\sin\phi_r - h.\ddot{\phi}_r.\cos\phi_r$; A_y is the lateral acceleration; $I_{xx,yy,zz}$ are the moments of inertia about the respective axes; u is the bus's longitudinal velocity; v is bus's lateral velocity.

The vertical dynamics of the sprung mass can be shown as

$$\begin{aligned}m\ddot{z} &= m.\left(\dot{\phi}_r^2 h.\cos\phi_r + \ddot{\phi}_r h\sin\phi_r\right) \\ &= \left(F_{zL} + F_{zR}\right) - mg.\cos\phi_r\end{aligned} \tag{3}$$

where m is the sprung mass; A_y is the lateral acceleration.

If the road bank angle is zero, (1)–(3) can be expressed as follows:

$$\sum F_y = m.\left(\dot{v} + ru + h\gamma^2.\sin\phi_r + h\dot{\phi}_r{}^2.\sin\phi_r - h\ddot{\phi}_r.\cos\phi_r\right) \tag{4}$$

$$\begin{aligned}&\left(I_{xx} + mh^2\right).\ddot{\phi}_r = \left(F_{zL} - F_{zR}\right).\frac{d}{2} + \ldots\sum F_y.h.\cos\phi_r \\ &+ mgh.\sin\phi_r + \left[\left(I_{yy} - I_{zz}\right) - mh^2\right].\gamma^2.\sin\phi_r.\cos\phi_r\end{aligned} \tag{5}$$

$$m\ddot{z} = m.\left(\dot{\phi}_r^2 h.\cos\phi_r + \ddot{\phi}_r h\sin\phi_r\right) = \left(F_{zL} + F_{zR}\right) - mg \tag{6}$$

The LTR, which estimates the difference in the tire's normal forces acting on each side of the bus, is a commonly used load transfer metric [14]. Equation (7) gives the expression of the LTR:

$$\mathrm{LTR} = \left|\frac{F_{zR} - F_{zL}}{F_{zR} + F_{zL}}\right| \tag{7}$$

where F_{zR} and F_{zL} represent the vertical force of the right tire and the left tire, respectively, and $F_{zR} + F_{zL} = mg$. The LTR varies from 0 to 1, where 1 represents one side of bus tires losing contact with the ground.

Solving the simultaneous equations, assuming that $\ddot{\phi}_r$ and $\dot{\phi}_r$ are zero and substituting them into (7), the following LTR expression is obtained, as shown below:

$$\begin{aligned}&LTR \\ &= \left|\frac{2}{d}.\frac{h.\left(\cos\phi_r.\left(\dot{v} + \gamma u\right) + h\gamma^2.\sin\phi_r + g.\sin\phi_r\right)}{g}\right|\end{aligned} \tag{8}$$

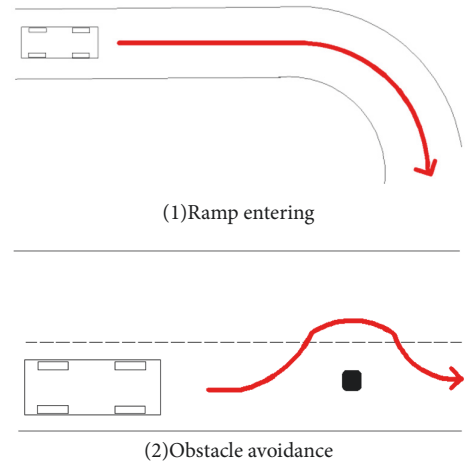

Figure 3: Bus rollover conditions.

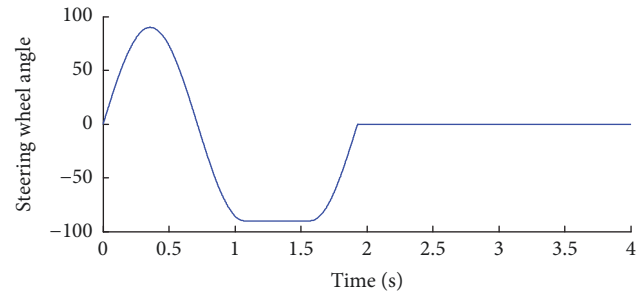

Figure 4: Steering wheel angle with 89 km/h Sindwell at 90° steering amplitude.

Further assumptions were adopted as follows: $\cos^2\phi_r \approx 1$, $h\gamma^2 \approx 0$, and $\dot{v} + \gamma u = A_y \cdot \cos\phi_r$ Therefore, the final expression of the estimated LTR is

$$LTR_e = \left|\frac{2h}{dg}\left[A_y + g.\sin\phi_r\right]\right|. \tag{9}$$

The results using (9) were abbreviated as Est-LTR. A built-in bus model provided by TruckSim can output each tire's vertical force; thus, the real LTR value can be calculated by (7) with these tire forces. The calculated result of (7) was referred to as the actual LTR, abbreviated as Act-LTR.

Some parameters of the bus are listed in Table 1.

To verify the effectiveness of (9), simulation works were carried out by comparing the estimated LTR (Est-LTR) and the actual LTR (Act-LTR) models. The road adhesion coefficient was set as 0.85, ensuring the lateral risk of rollover, but not of lateral slip. Figure 3 shows the common situations in which the rollover happens easily. In order to simulate these two conditions, we used the more complex maneuvers of Sindwell and DLC, which are often utilized for vehicles' lateral performance tests, to reproduce the rollover situations.

Figure 4 shows the steering angle of the 89-km/h Sindwell test where the steering amplitude was 90°. Results of the comparison under this test are demonstrated in Figure 5, which indicate that the trends of the two curves matched well. Figure 6 illustrates the steering wheel angle of the DLC

Table 1: Some parameters of the bus in TruckSim.

Sprung mass (m/kg)	7690
Bus width (d/m)	1.93
Distance from the sprung mass CG to the assumed roll axis (h/Vertical/m)	0.563

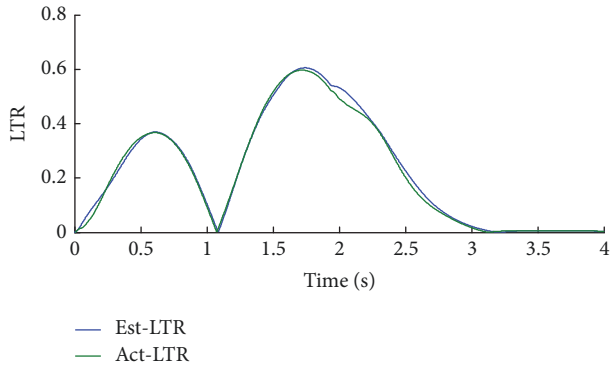

Figure 5: Estimated versus TruckSim load transfer ratio (LTR) with 89 km/h Sindwell at 90° steering amplitude.

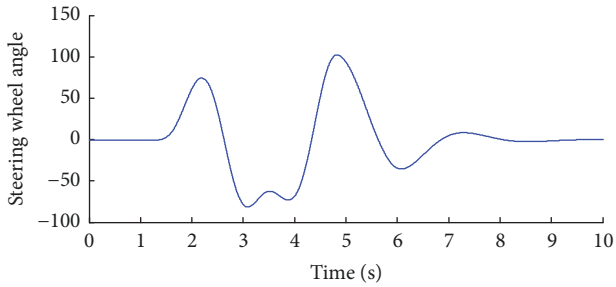

Figure 6: Steering wheel angle with 105 km/h double lane change (DLC).

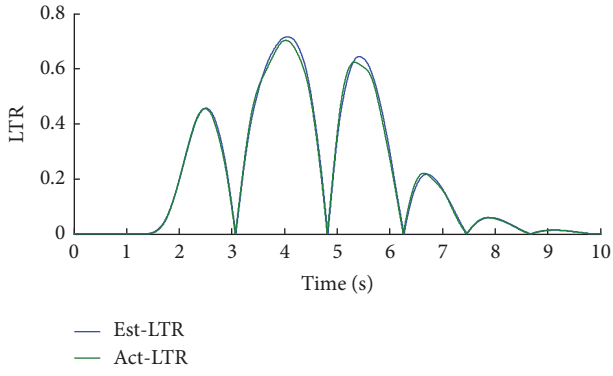

Figure 7: Estimated versus TruckSim LTR with 105 km/h DLC.

test, which was conducted according to ISO 3888-2:2002 [15]. Figure 7 demonstrates the comparison of the Est-LTR and Act-LTR under a test of a 105-km/h DLC; the figure indicates a slight lead time, with the Est-LTR reaching 0.7 at 3.841 s and Act-LTR reaching at 3.852 s. Hence, the estimation equation was valid as the reference formulation for a rollover prevention system. As a result, in the following sections, we considered the Est-LTR as the actual LTR.

2.2. Tire Model. To calculate the tire forces, this study utilized the Dugoff tire model, which is a nonlinear tire model. Compared with some empirical tire models, such as the "magic formula" (MF) model, which require a large number of tire-specific parameters that are probably unknown, the Dugoff model, by simple equations, can acquire the longitudinal and lateral tire-road forces under different wheel slip conditions [16].

Lateral and longitudinal tire-road forces can be defined as

$$F_{yi} = \frac{C_{yi}\tan\alpha_i}{1-\lambda_i} f(S)$$

$$F_{xi} = \frac{C_{xi}\lambda_i}{1-\lambda_i} f(S)$$

$$S = \frac{\mu F_{zi}}{2\sqrt{C_{xi}^2\lambda_i^2 + C_{yi}^2\tan^2\alpha_i}}\left(1-\lambda_i^2\right) \tag{10}$$

$$f(S) = \begin{cases} 1 & S > 1 \\ S(2-S) & S < 1. \end{cases}$$

C_{xi} and C_{yi} are the longitudinal and lateral corner stiffness of the tire, μ is the road adhesion coefficient maximum friction coefficient, λ_i is the slip ratio, and a_i is the slip angle of the wheels. In this study, the value of μ is 0.85; therefore, the bus lateral motion risk is the rollover rather than sideslip. The longitudinal wheel slip ratio λi can be obtained from TruckSim.

3. LTR Prediction Methodology

3.1. Grey Model. Among the grey model types, the one suitable for LTR prediction is the GM(1, 1) type, meaning "first-order one variable" [9]. This model is a time series forecasting model. The differential equations of the GM(1, 1) model are renewed as data becomes available to the prediction.

The grey prediction model's advantage is that just a few discrete data are necessary to characterize an unknown system. The GM(1, 1) steps are as follows [17]:

(1) Sort the initial series of $X(0)$ as $X^{(0)} = (X^{(0)}(1), X^{(0)}(2), X^{(0)}(3), \ldots, X^{(0)}(n))$. $X(0)$ is the series of LTR values that can be obtained by the tapped delay block in Simulink. In this study, we set n as equal to 10.

(2) Generate the first-order accumulated generating an operation (1-AGO) sequence. The general form of $X^{(1)}$ is

$X^{(1)}(1), X^{(1)}(2), X^{(1)}(3), \ldots, X^{(1)}(n)$ and the definition of 1-AGO of $X^{(0)}$ is

$$X^{(1)}(k) = \sum_{i=1}^{k} X^{(0)}(i) = X^{(1)}(k-1) + X^{(0)}(k). \quad (11)$$

(3) Set the first-order original differential equation of $X(1)$. Suppose $X(1)$ meets the equation below:

$$\frac{dX^{(1)}}{dt} + aX^{(1)} = b \quad (12)$$

This is the basic form of GM(1, 1), where variable a and variable b are coefficients. Define variable $\widehat{a} = [a, b]^T$.

Its difference equation is

$$X^{(0)}(k) + aZ^{(1)}(k) = b \quad k = 2, 3, \ldots, n. \quad (13)$$

$Z^{(1)}(k)$ is called the background value, and its equation is $Z^1(k) = \alpha X^1(k-1) + (1-\alpha)X^1(k)$.$\alpha$ is often set to 0.5. Therefore, according to the roots of this differential equation, the particular solution of (10) can be described as

$$\widehat{X}^{(0)}(k) = \left(X^{(0)}(1) - \frac{b}{a}\right)e^{-ak} + \frac{\mathrm{b}}{a} \quad (14)$$

where $\widehat{X}^{(0)}(k)$ is the predictive value of the series.

(4) Use the least square to obtain parameters a and b. Equation (15) can be written as

$$X^{(0)}(k+1) = a\left[-\frac{1}{2\left(X(1)(k+1) + X(1)(k)\right)}\right] + b, \quad k \geq n \quad (15)$$

$$\left[\frac{a}{b}\right] = \left(B^T B\right)^{-1} B^T Y_n,$$

where

$$B = \begin{bmatrix} -\left(X^{(1)}(1) + X^{(1)}(2)\right) \\ -\left(X^{(1)}(2) + X^{(1)}(3)\right) \\ \cdots \\ -\left(X^{(1)}(n-1) + X^{(1)}(n)\right) \end{bmatrix} \quad (16)$$

and

$$\mathrm{Yn} = \left(X^{(0)}(2), X^{(0)}(3), \ldots, X^{(0)}(n)\right) \quad (17)$$

(5) Estimate the AGO value $\mathrm{X}^1(1)$ and insert a and b into (8) in order to obtain the particular solution of the differential equation.

As a result, the recovery of the predictive value can be acquired by the following equation:

$$\widehat{X}^{(0)}(k) = \widehat{X}^{(1)}(k) - \sum_{i=1}^{k-1} \widehat{X}^{(0)}(i) \quad (18)$$

3.2. Buffer Operator. During some severe handling tests, the LTR value changes rapidly. This results in the predictive values growing fast and causing unintended local peaks in the prediction curve. For this reason, it is necessary to mitigate the growth trend among the time sequence to obtain smooth predictive curves.

X(0) is the delayed LTR data series, D is the grey buffer operator applied to X(0), and XD = (X(1)d1, X(2)d2, ..., X(n)dn) is the sequence after the function of the operator D on X. D is called the sequence operator and XD is the first-order operator acting sequences $D = (d1, d2, \ldots, dn)$.

Basic knowledge about the weakening buffer operator: when D meets the three conditions below, D can be called a weakening buffer operator [18]; otherwise, it cannot be:

(a) If X is a monotonic increasing series:

B is a weakening buffer operator $\Longleftrightarrow$ X(k)≤ $\mathrm{X(k)d_k}$

(b) If X is a monotonic decreasing series:

D is a weakening buffer operator $\Longleftrightarrow$ X(k)≥ $\mathrm{X(k)d_k}$

(c) If X is a vibrational series:

$$\min_{1\leq k\leq n}\{x(k)\} \leq \min_{1\leq k\leq n}\{x(k)\,d_k\}$$
$$\text{and } \max_{1\leq k\leq n}\{x(k)\} \geq \max_{1\leq k\leq n}\{x(k)\,d_k\} \quad (19)$$

D is a weakening buffer operator.

In this study, a buffer operator was utilized as below:

$X(k)D = (X(n))\rho(X(k))(1-\rho), k = 1, 2, 3, \ldots, n$; D is a buffer operator and ρ is the weight of X(n). In this paper, the prediction results could reach a balance between the ideal lead time and the smoothness of the prediction curve when the value of the weight variable ρ was 0.8.

3.3. Real-Time LTR Prediction. The simulation works of LTR prediction were implemented in the TruckSim and Simulink co-atmosphere. The TruckSim software can provide a built-in bus model with dynamic outputs that are very close to the filtered data acquired from a real running bus. Figure 8 shows the LTR prediction process using the grey model, which is an open loop. The lateral acceleration and roll angles $-A_y$ and ϕ_r were exported in real time from TruckSim and then utilized by the LTR equation to obtain an estimated LTR. The tapped delay block was utilized to delay and save the LTR values of a continuous time period, and the LTR series was sent to the next process. At first, 10 continuous data were acquired in real time. To avoid the results being infinity or not being a number, we set the initial LTR data as 0.01. We used a heuristic method to find that 10 was a suitable number. If n is over 10, the series contains too much old information which will have a side effect on the prediction result; if n is less than 10, the number is not enough to give a reasonable prediction result. Before the grey model process, the buffer operator was used on $(X^{(0)}(1), X^{(0)}(2), \ldots, X^{(0)}(n))$

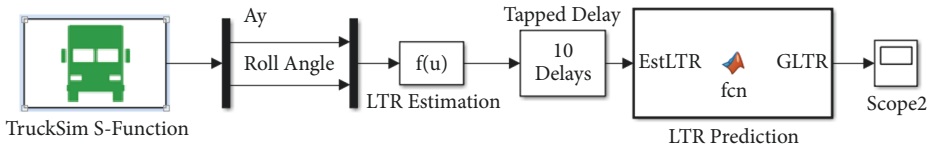

Figure 8: LTR prediction process.

and the buffered sequence $D*(X^{(0)}(1), X^{(0)}(2), \ldots, X^{(0)}(n))$ was generated. On the basis of the new sequence, the five steps of GM(1, 1) were implemented to get the predicted series $(\widehat{X}^{(0)}(1), \widehat{X}^{(0)}(2), \ldots, \widehat{X}^{(0)}(n), \ldots, \widehat{X}^{(0)}(n+f))$, and $\widehat{X}^{(0)}(n+f)$ is the predicted LTR value. During the predicted sequence, the preferred lead time is f∗Ts, where f and Ts represent the forward steps and the sample interval separately. Hence, if it is assumed that Ts is 0.02 s and f is 10, then the preferred lead time is 0.2 s. After the grey model process, the future LTR was obtained and stood as the reference value of earlier rollover detection. When a processing cycle ends, the old data are released, and a new cycle begins. The predicted LTR value produced by the grey model is called the GLTR.

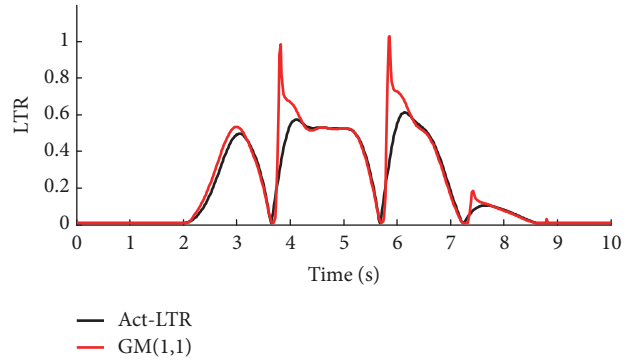

Figure 9: Prediction results in 85-km/h DLC using GM(1, 1).

4. LTR Prediction Results

To examine how long the lead time can be generated by the GLTR index, some comparison simulations are reported in this section. Under the cosimulation atmosphere, high-risk rollover maneuvers were carried out to examine the different performances between the GLTR and LTR. The chosen tests were the Sindwell and DLC maneuvers. Sindwell is a typical maneuver for testing a vehicle's lateral performance, which was established by the National Highway Traffic Safety Administration (NHTSA). Concurrently, the double lane change maneuver has been adopted by many vehicle companies as another typical lateral procedure.

In this part, the forward prediction steps were all 10, and the interval time was 0.02 s. As a result, the corresponding preferred lead time was 0.2 s.

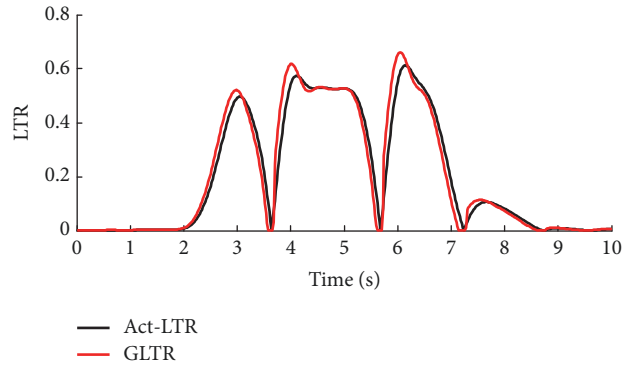

Figure 10: Prediction result for 85-km/h DLC using the grey LTR (GLTR).

4.1. Limiting Factor of GM(1,1). This part discusses the LTR prediction results without the buffer operator process. The prediction results for more complex handling tests such as the DLC and Sindwell tests proved that GM(1, 1) had a severe limitation. The drawback was that if the predicted LTR was saturated by the physical threshold, the algorithm may generate a wrong warning or activate the control system, even at a safe driving speed.

To demonstrate this issue, a typical example of the 85-km/h DLC test is presented in Figure 9. During this maneuver, the LTR threshold we set for rollover prevention was 0.7. Nevertheless, the actual LTR was about 0.6, meaning that there was no actual rollover risk. Under this practical circumstance, there is no need to initiate the rollover prevention systems at this relatively safe driving speed. However, the peak points of the prediction curves were (3.82, 0.985) and (5.86, 1.031), which were all above the threshold. Due to the peak point being over 0.7, the prediction curve will lead to the unnecessary initiation of the prevention system.

As a result, particularly at a lesser high speed, the use of basic GM(1, 1) in the LTR prediction has limiting factors in serious rollover risk conditions where these prediction mutations will cause the unintended initiation of the rollover prevention system. This limiting factor prevents the grey model from extending its application to the entire speed range.

To overcome this issue, first, the trend development in the old data series needed to be reduced. As shown in Figure 10, we used a buffer to shrink the data tendency before we applied GM(1, 1) to the real-time data series. Therefore, after combining GM(1, 1) with the proposed buffer, the GLTR algorithm was formed.

Figure 10 displays the effectiveness of the GLTR in the 85-km/h DLC test. Compared with Figure 9, the weakening effect was obvious, causing the peak position to reduce from (5.86, 1.031) to (6.04, 0.661), which was very close to the peak position (6.14, 0.623) of the Est-LTR. As a result, after the

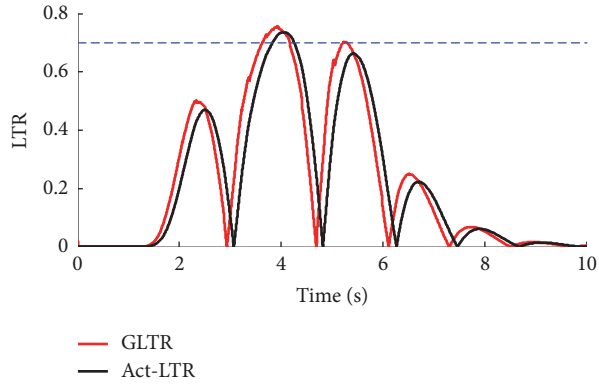

Figure 11: Prediction results for the 105-km/h DLC test.

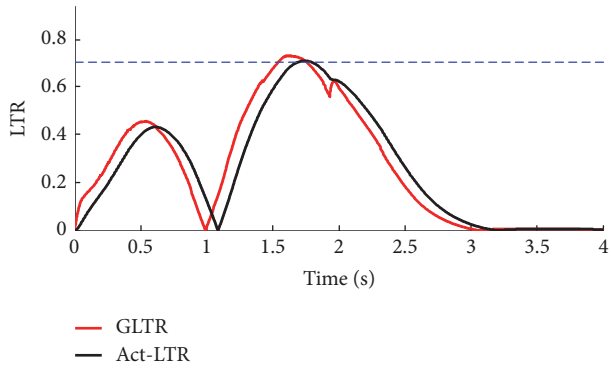

Figure 12: Prediction results for the 89-km/h Sindwell test.

Table 2: Prediction of GLTR efficacy.

Tests	T1	T1'	ΔT1
A. 105 km/h DLC	3.841 s	3.634 s	0.207 s
B. 89 km/h Sindwell	1.698 s	1.521 s	0.177 s

addition of a buffer operator, the GLTR can overcome the limiting factor of GM(1, 1) by giving a reasonable prediction performance at a secondary high speed for rollover-risk maneuvers.

4.2. Prediction Results of the GLTR. In order to verify the effectiveness of the GLTR for the target lead time, 105-km/h DLC and 89-km/h Sindwell simulation tests were conducted using the GLTR index. The prediction results of these two maneuvers are shown in Figures 11 and 12. T1 and T1' are the time points at which the Est-LTR and the GLTR reach the threshold. Table 2 provides a detailed description of the prediction results for these two maneuvers where the lead times were substantial. During the 105-km/h DLC, with the rollover threshold set as 0.7, the lead time was 0.207 s. Concurrently, during the 89-km/h Sindwell, the lead time was 0.177 s.

Therefore, after applying the GLTR index, with the sufficient lead time, the activation command could be triggered in advance about 0.2 s. GLTR performed better than GM(1, 1) in LTR prediction by acquiring enough lead time and reducing the prediction crests. Furthermore, the new threshold signal can be useful for additional warning systems or differential-based systems, which will highly reduce the rollover risks.

To further illustrate the efficacy of the GLTR, the results were compared with other works. We still use a 89-km/h Sindwell maneuver as an example. In [19], a predictive LTR index PLTR was introduced. Equation (20) is the basic expression for the PLTR. In the test, future time Δt is 0.2 s, corresponding to the preferred lead time in this study.

$$PLTR_{t0}(\Delta t) = LTR(t0) + \dot{LTR}(t0) \cdot \Delta t \tag{20}$$

The lead time of PLTR was 0.163s, which is less than 0.177s (using GLTR), proving GLTR's efficacy.

5. Further Verification

In addition, to further examine the actual effectiveness of this new rollover index, a Simulink model (an active differential braking system) was added to function as the rollover prevention system. GLTR works as the threshold of the rollover prevention action. Figure 13 shows the control structure of the differential braking system. Once the system detects that the GLTR has exceeded the threshold, the actuator will begin to provide differential braking forces as the yawing moment intervention. F_{flb}, F_{frb} are the front left and front right braking forces. F_{rlb}, F_{rrb} are the rear left and rear right braking forces. Once GLTR is over 0.7, the antirollover countermeasure begins by adding an additional yawing moment.

A 2-DOF vehicle model, which is the so-called "bicycle model", was used as the reference model.

Based on the 2-DOF model and Formula (10), the reference yawing moment can be calculated as below:

$$\sum M_{zr} = aF_{y1} - bF_{y2} = aC_{y1}\alpha_1 - bC_{y2}\alpha_2 \tag{21}$$

Therefore, the additional moment can be obtained by the equation as below:

$$\Delta Mz = M_z - M_{zr} \tag{22}$$

The differential braking is achieved by establishing a PID controller. A proportional–integral–derivative controller (PID controller) is a control loop feedback mechanism widely used in industrial control systems and a variety of other applications requiring continuously modulated control [20]. The distinguishing feature of the PID controller is the ability to use the three control terms of the proportional, integral, and derivative influence on the controller output to apply accurate and optimal control.

The overall control function can be expressed mathematically as

$$U(s) = K_p\left(1 + \frac{1}{k_i.s} + K_d.s\right).E(s) \tag{23}$$

where

Kp is the proportional gain, a tuning parameter,

K_i is the integral gain, a tuning parameter,

K_d is the derivative gain, a tuning parameter.

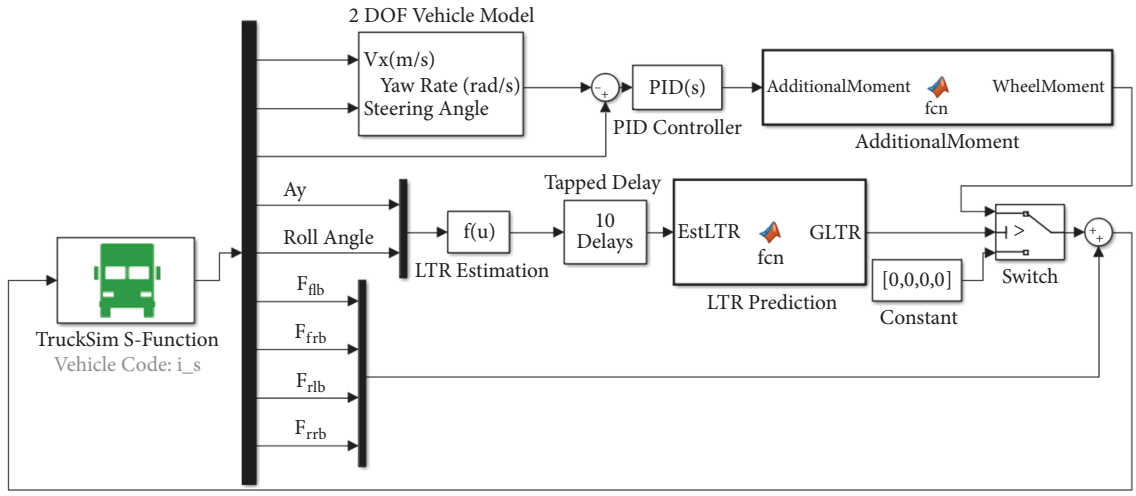

Figure 13: GLTR control system using PID controller.

$E(s) = \gamma_e - \gamma_r$ is the error of yaw rate, where γ_e and γ_r are the measured raw rate and reference yaw rate.

We used the yaw rate error as the control goal to calculate the target yawing moment. In (23), $K_p = 290$, $K_i = 120$, and $K_d = 2.4$.

According to steering characteristic of a bus, Table 3 is listed for the selection of the braking wheel to achieve the required yawing moment.

To better understand the effectiveness of GLTR, estimated LTR was also used as the threshold in the comparison simulation tests. This simulation tested the performances of the prevention system after the application of the GLTR and LTR.

This part demonstrates the simulation results acquired from the closed-loop cosimulation utilizing the GLTR index studied in this paper. The cosimulation model included the bus model in TruckSim, an active differential braking system built in Simulink. The active differentials obtained opposite moment by adding extra braking torque on a certain wheel, so that the vehicle was able to effectively control the roll and yaw motions.

We used LTR and GTR as the threshold in the controllers separately. To validate the GLTR, comparison simulation tests were carried out with TruckSim to find the impact of the new controller. The comparison was conducted among a bus with the control system off, a bus with the LTR active, and a bus with the GLTR active. The simulation test was for the 100-km/h "Sindwell" maneuver with a 90° amplitude. First, Figure 14 shows the LTR prediction result using LTR. The peak points of LTR and GLTR curves are (1.608, 0.775) and (1.802, 0.758), where there are 0.2 s between the two peak points.

From Figure 15, the buses with the LTR and the GLTR matched well until the midpoint of the second turn when the GLTR systems activated prior to the LTR. The peak points of GLTR control and LTR control were reduced to (1.639, 0.671) and (1.727, 0.691) separately. We could see that the GLTR control could help the bus reach a steady state prior to the bus under LTR control. The two curves reached zero at 2.55 s and 2.72 s, showing that the GLTR control could make the bus steady 0.17 s in advance.

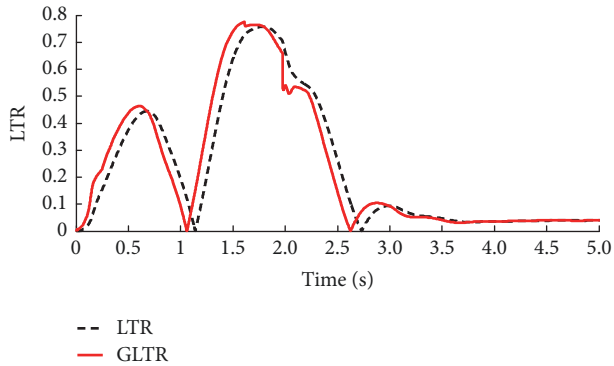

Figure 14: Prediction results for the 100-km/h Sindwell test.

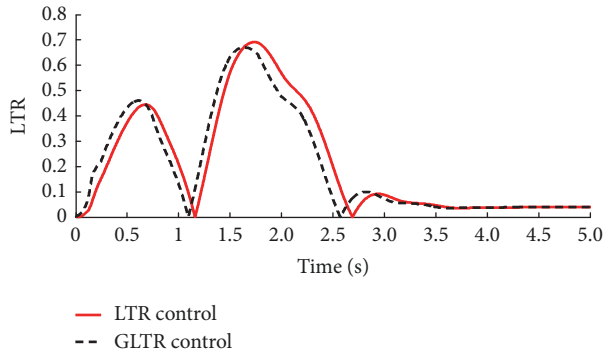

Figure 15: Comparison result in the 100-km/h Sindwell test using differential controllers.

Figure 16 shows the comparison result of the roll angles between the LTR control and GLTR control. The GLTR could help the bus reduce the yawing rate about 0.035 rad/s, remarkably reducing the possibilities of rollover.

Table 3: Braking strategy of a bus.

Steering angle	$\Delta\gamma$	Steering property	Braking wheel
> 0	> 0	oversteer	Right front
	< 0	understeer	Left rear
< 0	> 0	understeer	Right rear
	< 0	oversteer	Left front

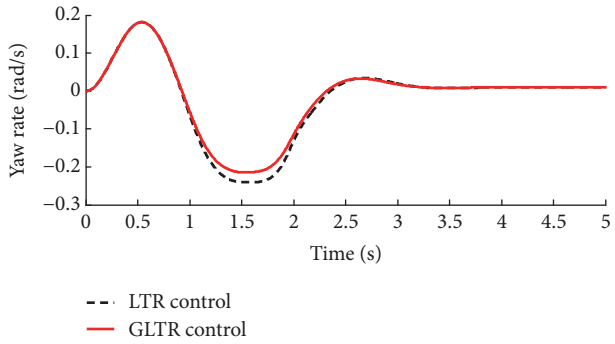

Figure 16: Comparison result of the yaw rate in the 100-km/h Sindwell test.

6. Conclusions

This study demonstrated an LTR prediction algorithm for bus rollover systems. Unlike existing methods that are based on estimation algorithms, the proposed algorithm could generate a considerable lead time for rollover prevention systems or warning systems. This rollover index was the fusion of the grey model and a buffer operator that was introduced for bus rollover detection. The simulation study aimed at examining the prediction effectiveness of the GLTR and its application possibility. Some conclusions regarding this approach can be made as follows.

(1) An LTR estimation equation was developed and then verified to have a rather suitable agreement with the LTR definition formula that directly makes use of the vertical tire forces from TruckSim.

(2) Lead times produced by the GLTR help the warning systems activate in advance, which will reduce the possible risks of bus rollover.

(3) Further simulation verification was carried out by applying the GLTR in a differential-based system. Compared with the traditional LTR index, the GLTR could help the differential-based system have better performance and efficacy.

(4) In the future, for further promotion, this new rollover index should be applied to a real rollover prevention system to conduct hardware in loop tests or road assessments.

Data Availability

The data used to support the findings of this study are available from the corresponding author upon request.

Conflicts of Interest

The authors declare that there are no conflicts of interest regarding the publication of this paper.

Acknowledgments

This work is supported by National Natural Science Foundation of China (Grant No. 51278062).

References

[1] V. Eyges, J. Padmanaban, and G. Stadter, "A comparative study of rollover crashes involving passenger cars with and without electronic stability control (ESC)," *SAE Technical Papers*, 2011.

[2] M. E. Greene and V. S. Trent, "A predictive rollover sensor," *SAE Technical Papers*, 2002.

[3] R. D. Ervin, "The influence of size and weight variables on the roll stability of heavy duty trucks," *SAE Technical Papers*, 1983.

[4] H. Yu, L. Güvenç, and Ü. Özgüner, "Heavy duty vehicle rollover detection and active roll control," *Vehicle System Dynamics*, vol. 46, no. 6, pp. 451–470, 2008.

[5] S. Solmaz, M. Akar, and R. Shorten, "Adaptive rollover prevention for automotive vehicles with differential braking," *IFAC Proceedings Volumes*, vol. 41, no. 2, pp. 4695–4700, 2008.

[6] A. Mayr, G. Klambauer, T. Unterthiner et al., "Large-scale comparison of machine learning methods for drug target prediction on ChEMBL," *Chemical Science*, vol. 9, no. 24, pp. 5441–5451, 2018.

[7] Z. Liu, H. Li, K. Liu, H. Yu, and K. Cheng, "Design of high-performance water-in-glass evacuated tube solar water heaters by a high-throughput screening based on machine learning: A combined modeling and experimental study," *Solar Energy*, vol. 142, pp. 61–67, 2017.

[8] Y. Cheng, F. Wang, P. Zhang, and J. Hu, "Risk Prediction with Electronic Health Records: A Deep Learning Approach," in *Proceedings of the 2016 SIAM International Conference on Data Mining*, pp. 432–440, 2016.

[9] J. L. Deng, "Introduction to grey system theory," *The Journal of Grey System*, vol. 1, no. 1, pp. 1–24, 1989.

[10] M. Mao and E. C. Chirwa, "Application of grey model GM(1,1) to vehicle fatality risk estimation," *Journal of Technological Forecasting & Social Change*, vol. 73, no. 5, pp. 588–605, 2006.

[11] A. Manivanna Boopathi and A. Abudhahir, "Design of grey-verhulst sliding mode controller for antilock braking system," *International Journal of Control, Automation, and Systems*, vol. 14, no. 3, pp. 763–772, 2016.

[12] S.-J. Huang and S.-T. Chao, "A new lateral impact warning system with grey prediction," *Proceedings of the Institution of Mechanical Engineers, Part D: Journal of Automobile Engineering*, vol. 224, no. 3, pp. 285–297, 2010.

[13] T. Chou and T.-W. Chu, "An improvement in rollover detection of articulated vehicles using the grey system theory," *Vehicle System Dynamics*, vol. 52, no. 5, pp. 679–703, 2014.

[14] J. Preston-Thomas and J. H. F. Woodrooffe, "Feasibility Study of a Rollover Warning Device for Heavy Trucks," *Transport Canada*, 1990.

[15] S. Wood, *Passenger Cars—Test Track for a Severe Lane-Change Maneuver—Part 2: Obstacle avoidance*, The international organization for standardization, 2011.

[16] T. Hsiao, "Robust estimation and control of tire traction forces," *IEEE Transactions on Vehicular Technology*, vol. 62, no. 3, pp. 1378–1383, 2013.

[17] S. F. Liu and Y. Lin, *Grey Systems: Theory and Applications*, Springer, Berlin, Germany, 2010.

[18] L. F. Wu, S. F. Liu, Y. J. Yang, L. Ma, and H. Liu, "Multi-variable weakening buffer operator and its application," *Information Sciences*, vol. 339, pp. 98–107, 2016.

[19] C. Larish, D. Piyabongkarn, V. Tsourapas, and R. Rajamani, "A new predictive lateral load transfer ratio for rollover prevention systems," *IEEE Transactions on Vehicular Technology*, vol. 62, no. 7, pp. 2928–2936, 2013.

[20] K. H. Ang, G. Chong, and Y. Li, "PID control system analysis, design, and technology," *IEEE Transactions on Control Systems Technology*, vol. 13, no. 4, pp. 559–576, 2005.